J Supercond Nov Magn (2015) 28:331–337
DOI 10.1007/s10948-014-2700-3

ORIGINAL PAPER

Microwave Conductivity in Two-Band Superconductors $V_{3+x}Si_{1-x}$

Oleg V. Dolgov · Alexander A. Golubov · Yuri A. Nefyodov · Alexei M. Shuvaev · Mikhail R. Trunin

Received: 9 June 2014 / Accepted: 11 August 2014 / Published online: 26 August 2014

Abstract We present the results of investigations of the temperature dependences of complex conductivity $\sigma(T) = \sigma'(T) - i\sigma''(T)$ at frequency 9.4 GHz in series of single crystals $V_{3+x}Si_{1-x}$ with different Si content. The data exhibit peculiarities typical for multiband superconductors, namely a nonlinear temperature dependence of resistivity above superconducting transition temperature T_c, suppression of superconducting transition temperature T_c by nonmagnetic impurities, a positive curvature of $\sigma''(T)$ curves close to T_c, and a coherence peak in $\sigma'(T)$ at $T \sim T_c/2$. Using a two-band model in the weak-coupling regime, we demonstrate that the behavior of T_c and the evolution of $\sigma(T)$ with Si-content variation are consistently described by changing of the interband scattering rate.

O. V. Dolgov
Max Planck Institute for Solid State Research, Stuttgart, Germany

O. V. Dolgov
P.N. Lebedev Physical Institute RAS ,Moscow, Russia

A. A. Golubov
Faculty of Science and Technology and MESA+ Institute of Nanotechnology, Enschede, Netherlands

A. A. Golubov · M.R. Trunin
Moscow Institute of Physics and Technology, Dolgoprudny, Moscow Russia

Yu.A. Nefyodov · M.R. Trunin (✉)
Institute of Solid State Physics RAS, 142432 Chernogolovka, Moscow Russia
e-mail: trunin@issp.ac.ru

A.M. Shuvaev
Institute of Solid State Physics, Vienna University of Technology, 1040 Vienna, Austria

Keywords Microwave surface impedance · Complex conductivity of superconductors · BCS theory · Two-band model

1 Introduction

Possible existence of superconductors with different order parameters at the Fermi surface [1–3] was predicted soon after the microscopic theory of Bardeen-Cooper-Schrieffer (BCS) [4]. Recently, to explain the observed deviations from the predictions of the BCS theory, the realization of multiband superconductivity was suggested in a number of transition metals [5–7], Nb-doped $SrTiO_3$ [8], rare earth Ni-borocarbides [9], the layered superconductor $NbSe_2$ [10], as well as $MgNi_3C$ [11], heavy-fermion compounds $CeCoIn_5$ [12] and $CePt_3Si$ [13] and in Nb_3Sn [14]. Recently, manifestations of two-band superconductivity are discovered in superconductors with higher transition temperature T_c: MgB_2 ($T_c = 39$ K) where two superconducting gaps, Δ_π Δ_σ, are resolved in some experiments and iron-pnictides ($T_c \leq 50$ K) where the description of electronic transport and thermodynamical characteristics requires contribution of multiple bands which strongly differ by their kinetic properties (see recent reviews in [15, 16]).

At the same time, the situation with A15 compounds is still controversial. Studies of the temperature variation of a superfluid density [17, 18] and an optical conductivity [19] in A15-structure superconductor V_3Si have revealed well-resolved multiband features. On the other hand, the measurements of the thermal condictivity [10], of the field dependence of the magnetic field penetration depth [20], and of the reversible magnetization [21] were interpreted within the single-band scenario. In this contradictory situation, further studies of V_3Si are very important. In this work,

we present the results of experimental and theoretical study of magnetic penetration depth and microwave conductivity in $V_{3+x}Si_{1-x}$ single crystals with different Si content at frequency 9.4 GHz and demonstrate clear two-band features in the microwave response.

2 BCS Theory and Two-Band Model

Functional relationship between the measured surface impedance Z and conductivity σ in superconductors depends significantly on the dimensionless parameter $S = (E - \imath\gamma/2)/(qv_F)$ [22], where the parameters with dimension of energy E, γ, and qv_F have the following characteristic values: $E \approx \Delta$ is a gap value at $T = 0$ in the superconducting state and $E \approx 0$ in the normal state, $\gamma = 1/\tau$ is the inverse relaxation time of quasiparticles, v_F is the Fermi velocity, and q is the wave number that characterizes the range of electromagnetic field variation: $q \sim 1/\lambda$ in the superconducting state (λ is the magnetic field penetration depth) and $q \sim 1/\delta$ in the normal state (δ is skin depth). If $S \gg 1$, then the relation between the field and the current in a superconductor is local, while for $S \ll 1$, it is essentially nonlocal. In some cases, it is more convenient to compare these energy parameters with parameters that have the dimension of length, namely the mean free path $l = v_F/\gamma$, the coherence length $\xi_0 = v_F/(\pi\Delta)$, and the magnetic field penetration depth λ.

V_3Si crystals are in the London limit since the coherence length $\xi(0) \sim 10$ nm is much less than the magnetic field penetration depth $\lambda(0) \sim 100$ nm at $T = 0$, and therefore, the relationship between the current and field is local. In this case, the surface impedance $Z = R + iX$ defines the complex conductivity $\sigma = \sigma' - i\sigma'' = i\omega\mu_0/Z^2$, where $\omega = 2\pi f$ is the measurement frequency and $\mu_0 = 4\pi \cdot 10^{-7}$ H/m.

Figure 1 shows the calculated temperature dependences of the conductivity components $\sigma''(T)$ and $\sigma'(T)$ according to the formulas of the BCS theory as a function of the parameter $\omega\tau$ at fixed frequency $f = 10$ GHz. The conductivity values $\sigma''(0)$ decrease with increasing relaxation rate $\gamma = 1/\tau$, reflecting the increase of the penetration depth in a dirty London superconductor compared with a pure one (the left figure). The existence of a nonzero imaginary part of the conductivity in the normal state of pure superconductors associated with temporal dispersion of Drude conductivity $\sigma_0 = ne^2\tau/m$: $\sigma_n = \sigma_n' - \imath\sigma_n'' = \sigma_0/(1+\imath\omega\tau)$. On the right panel of Fig. 1, the BCS coherent peak near T_c in the real part $\sigma'(T)$ of conductivity is visible. In a London ($S \gg 1$) pure ($\gamma < \omega \ll \Delta$) superconductor, the coherent peak is absent. As the relaxation rate γ increases, the peak appears at $\gamma \geq \omega$ and increases in amplitude as long as the transition from pure ($\gamma < \Delta$) to dirty ($\gamma > \Delta$) limit occurs. Thereafter, coherent peak ceases to grow, reaching the value of order $\sigma'_{\max}/\sigma'(T_c) \sim \ln(\Delta/\omega)$ [22].

Two-band model of superconductivity assumes the presence of two coupled gap functions Δ_1 and Δ_2, which, in the weak-coupling regime, are described by the system of equations given in [23]. Let subscripts α and β take the values 1 or 2, corresponding to a number of an electronic band. The matrix of electron–boson interaction constants $\Lambda_{\alpha\beta}$ replaces Λ which determines the relation between transition temperature and characteristic cutoff frequency of a phonon spectrum ω_D in the single-band BCS theory: $T_c = (2\gamma^*\omega_D/\pi)\exp(-1/\Lambda)$ ($\gamma^* \approx 1.78$ is Euler's constant). Electronic scattering by nonmagnetic impurities is taken into account by scattering rates $\gamma_{\alpha\beta} = 1/\tau_{\alpha\beta}$, which in the considered weak-coupling regime do not depend on energy. Nondiagonal elements of the scattering and interaction matrices are related like $\gamma_{12}/\gamma_{21} = \Lambda_{12}/\Lambda_{21}$. Each of gap functions Δ_α found from the system of equations [23] is used to calculate microwave conductivity $\sigma_\alpha = \sigma'_\alpha - \imath\sigma''_\alpha$ for each band using the expressions for local (London) regime [22] derived in the single-band case. Total conductivity is determined by a sum of conductivities in each band taking into account partial plasma frequencies, ω_{pl1} and ω_{pl2}, without cross-terms, which is justified in the local limit [24].

In isotropic single-band superconductor, the presence of not too strong impurity concentration does not lead to changes of thermodynamic properties of a superconductor in particular its transition temperature. In multiband superconductors, the picture is quite different [23, 25]. In addition to intraband scattering processes of electrons (characterized by coefficients γ_{11} and γ_{22}), when electron remains in the same energy band after scattering process, there are scattering processes with interband transitions (characterized by coefficients γ_{12} and γ_{21}).

Assume that the superconducting gap in band 1 is larger than in band 2. The physical meaning of the parameters $\Lambda_{\alpha\beta}$ and $\gamma_{\alpha\beta}$ are as follows: Λ_{11} specifies the maximum value of T_c; Λ_{22} characterizes the low-temperature region $T < T_c/2$, in particular, the temperature dependences of the conductivity curves $\sigma'(T)$ and $\sigma''(T)$ at $T \to 0$; Λ_{12} and Λ_{21} should be much smaller than Λ_{11} or Λ_{22} to display the two-band superconductivity effects were pronounced; increasing of intraband scattering rates γ_{11} or γ_{22} reduce the effectiveness of electromagnetic field screening that appears to reduce the contribution of the imaginary part of conductivity $\sigma''(T)$ from the corresponding subband; increasing of γ_{21} tends to equalize the superconducting gaps in different bands, thus smoothing the temperature dependence of $\sigma''(T)$; and growth of γ_{12} leads to decrease T_c of superconductor almost without changing its other parameters. The latter effect, which occurs in multiband superconductors in contrast to single-band ones, is illustrated in

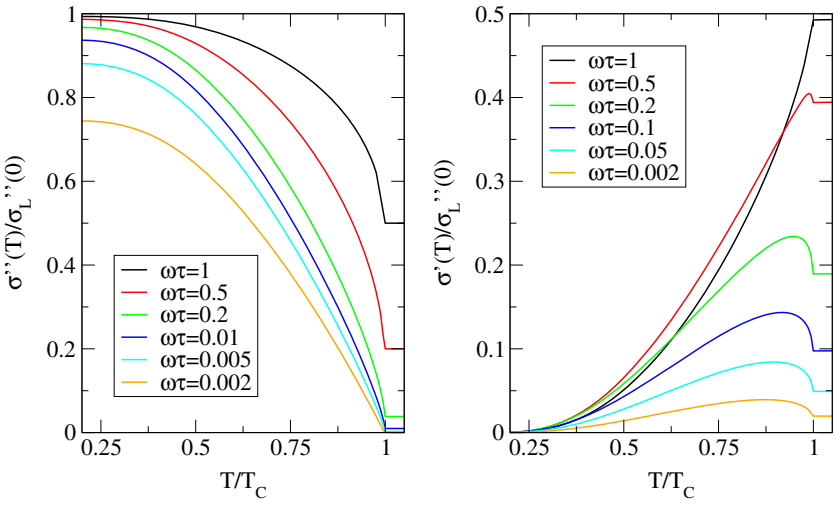

Fig. 1 Evolution of the temperature dependences of the microwave conductivity components within the framework of BCS theory and local electrodynamics. *Left* imaginary part of the conductivity. *Right* the real part. Both components are normalized to the value of the imaginary part of the conductivity at 0 temperature in pure limit $\sigma_L''(0)$

Fig. 2. With increasing γ_{12}, strongest suppression of superconductivity occurs in the band with larger gap as long as the gaps in the different bands are not equalized (Fig. 3). After that, the suppression of the critical temperature by interband scattering occurs less efficiently.

3 Comparison with Experiment

Crystals $V_{3+x}Si_{1-x}$ were grown by the method of zone melting in Ar atmosphere from polycrystalline blanks with pre-prepared composition which were also exposed to one pass zone melting in vacuum. For this study, selected five single-phase (i.e., consisting only the phase V_3Si) samples have been selected with Si-content 25, 24, 23, 22, and 21 atomic percent respectively. The samples have the form of thin plates with typical dimensions $2 \times 1 \times 0.5\text{mm}^3$. For all crystals, the width of the superconducting transition did not exceed 0.5 K, as is seen by measuring temperature dependences of their dynamic susceptibility.

For measurements of surface impedance components, we used the "hot finger" method. We placed the sample into the center of the cylindrical superconducting niobium cavity resonating at the frequency $f = \omega/2\pi =$

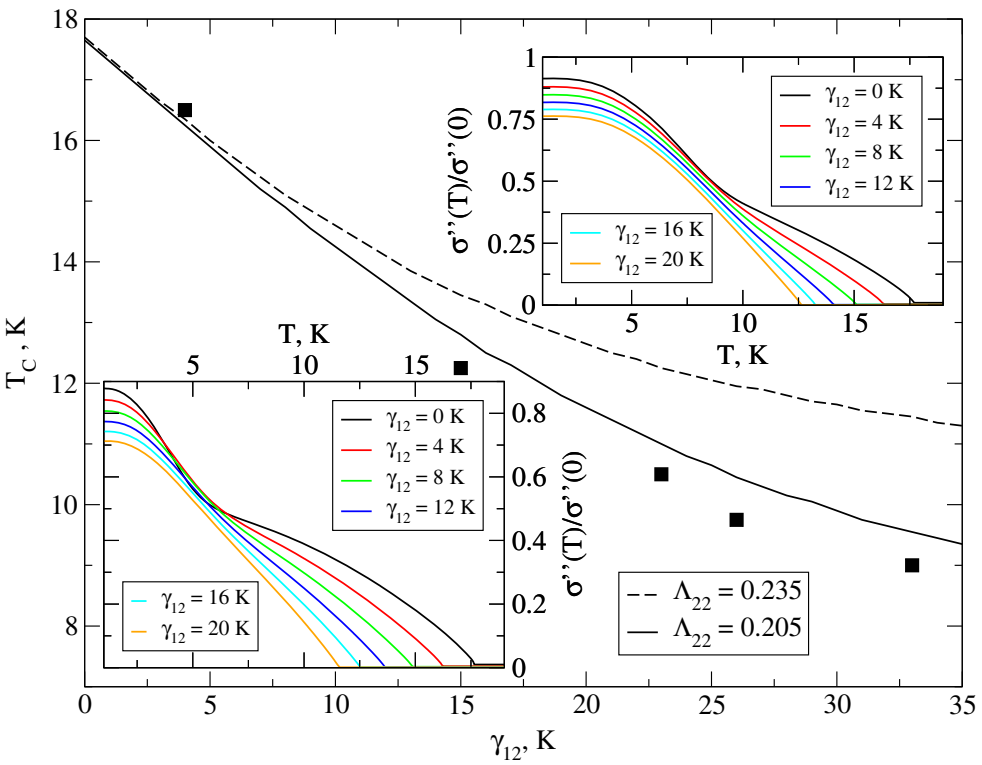

Fig. 2 Critical temperature T_c of two-band superconductor as a function of interband scattering rate γ_{12}. $\Lambda_{11} = 0.289$, $\Lambda_{12} = 0.006$, $\Lambda_{21} = 0.002$, $\gamma_{11} = \gamma_{22} = 5$ K, $\omega_{pl1} = \omega_{pl2}$, $\omega = 0.5$ K. The *solid line* shows the calculation for the case of $\Lambda_{22} = 0.205$ and *dashed line* for $\Lambda_{22} = 0.235$. *Squares* depict the experimental points (see the next section). The *insets* show the evolution of the curves $\sigma''(T)$ with changing γ_{12} (*bottom left curves* correspond to $\Lambda_{22} = 0.235$ and the *curves on the right at the top* to $\Lambda_{22} = 0.205$)

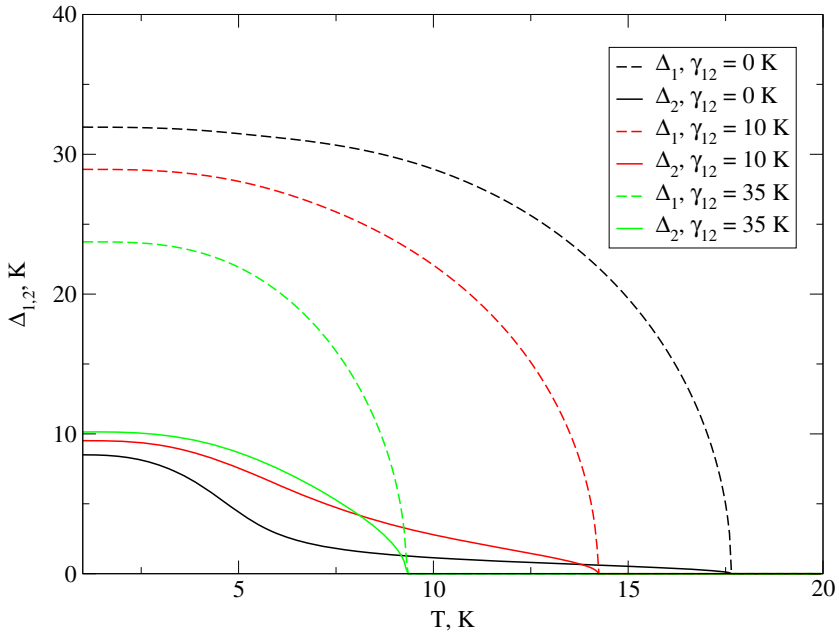

Fig. 3 Temperature dependences of the superconducting gaps on the interband scattering rates γ_{12}. Calculation parameters are the same as in Fig. 2 with $\Lambda_{22} = 0.205$

9.4 GHz in TE_{011} mode and having high unloaded quality factor $Q_0 \simeq 2 \times 10^7$. Since the sample is located at the antinode of the microwave magnetic field, the resonance frequency $f(T)$ of the system and its quality factor $Q(T)$ can be easily related to the surface impedance $Z(T) = R(T) + iX(T)$ of the sample using simple relations [26]. The real part of $Z(T)$, the surface resistance $R(T)$, is proportional to the microwave power absorbed by the sample, whereas the imaginary part, the surface reactance $X(T)$, is the reactive component which defines the electromagnetic field screening. In the superconducting state, $X(T)$ directly provides the magnetic field penetration depth $\lambda(T) = X(T)/\omega\mu_0$.

In the temperature range $2 \leq T \leq 20$ K, the results of measurements of the surface impedance components are shown in Fig. 4. For all samples, except for the stoichiometric one (25% of silicon), the normal skin effect condition, $R(T) = X(T)$, is satisfied at $T > T_c$. The reason for the discrepancy of $R(T)$ and $X(T)$ curves in the sample with the stoichiometric composition at $T_c < T < 30$ K is the

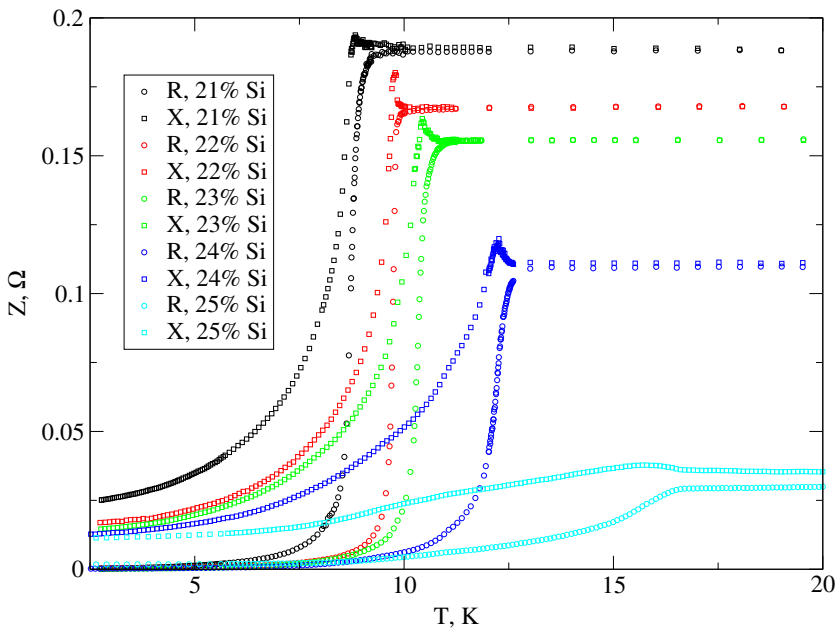

Fig. 4 Surface resistance $R(T)$ (*circles*) and reactance $X(T)$ (*squares*) of $V_{3+x}Si_{1-x}$ crystals with various Si content

Table 1 The parameters of the investigated crystals $V_{3+x}Si_{1-x}$

% Si	21	22	23	24	25
T_c, K	8.9	9.85	10.5	12.5	16.6
$\lambda(0)$, Å	3,260	2,160	1,860	1,640	1,520
γ_{12}, K	33	26	23	15	4
Λ_{22}	0.205	0.205	0.205	0.205	0.235

temporal dispersion of the Drude conductivity (estimated, $\omega\tau \approx 0.3$ for this sample). At higher temperatures $T > 30$ K, when the processes of electron-phonon scattering become significant and the relaxation time τ is reduced, the equality $R(T) = X(T)$ is also achieved in stoichiometric crystals [17].

The validity of the normal skin effect makes it possible to obtain the resistivities $\rho(T) = 2R^2(T)/\omega\mu_0$, as shown in Fig. 5. The data demonstrate strong deviations from the Bloch-Grüneisen behavior, namely the tendency to saturation of the resistivity at high temperatures. This behavior is very similar to that of the resistivity $\rho(T)$ in iron pnictide superconductors and can be explained within the two band scenario [27].

Table 1 shows the measured (critical temperature T_c and penetration depth $\lambda(0) = X(0)/\omega\mu_0$) and the fitting parameters γ_{12} and Λ_{22} of the investigated samples $V_{3+x}Si_{1-x}$. The constants of electron–phonon interaction Λ_{11}, Λ_{12}, Λ_{21} and the relative distribution of the electron within the subbands ω_{pl1} and ω_{pl2} are kept the same for all samples in the series, and the parameters Λ_{22}, $\gamma_{11} = \gamma_{22} = \gamma_{12}$ were adjusted for each sample. The last unknown parameter of interband scattering γ_{21} was calculated from the ratio of $\gamma_{21}/\gamma_{12} = \Lambda_{21}/\Lambda_{12}$ [23]. The best agreement with the experiment gives the values $\Lambda_{11} = 0.289$, $\Lambda_{12} = 6 \cdot 10^{-3}$, $\Lambda_{21} = 2 \cdot 10^{-3}$, $\omega^2_{pl1}/\omega^2_{pl2} = 0.07/0.93$, $\omega_D = 500$ K.

In Fig. 6, the symbols show the temperature dependences of the imaginary part of the microwave conductivity $\sigma''(T)$ in $V_{3+x}Si_{1-x}$ crystals normalized to its value at 0 temperature $\sigma''(0)$. These curves were obtained by the formulas of local electrodynamics $\sigma(T) = \sigma'(T) - i\sigma''(T) = i\omega\mu_0/Z^2(T)$ using the experimental dependences of the surface impedance shown in Fig. 4. All of them have a distinctive feature, namely the presence of near T_c region with positive curvature which is not explained in the framework of the single-band BCS model (dashed line in Fig. 6). Solid lines show the calculations within the two-band model of superconductivity. As seen from Fig. 6, the two-band model describes well the evolution of the experimental curves.

The temperature dependences of the real part of conductivity $\sigma'(T)$ are shown in Fig. 7. In all samples, except the stoichiometric (25% Si) one, the BCS coherent peak is observed. Unlike the single-band BCS theory in which the coherent peak occurs at $T \simeq 0.85T_c$, in Fig. 7, it is shifted to lower temperatures that is explained in the framework of two-band theory, namely the peak is formed by electrons from the subband with a smaller superconducting gap. The main difference between experimental and theoretical curves of $\sigma'(T)/\sigma'(T_c)$ consists in the amplitude of the coherent peak. The calculated peak amplitudes in Fig. 7 for all samples, except

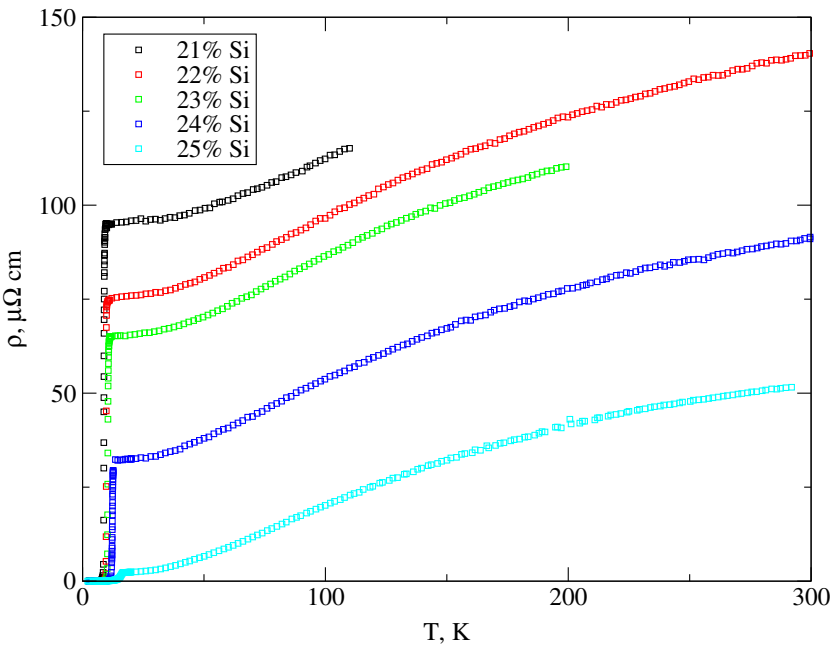

Fig. 5 Resistivities of $V_{3+x}Si_{1-x}$ crystals with various Si content

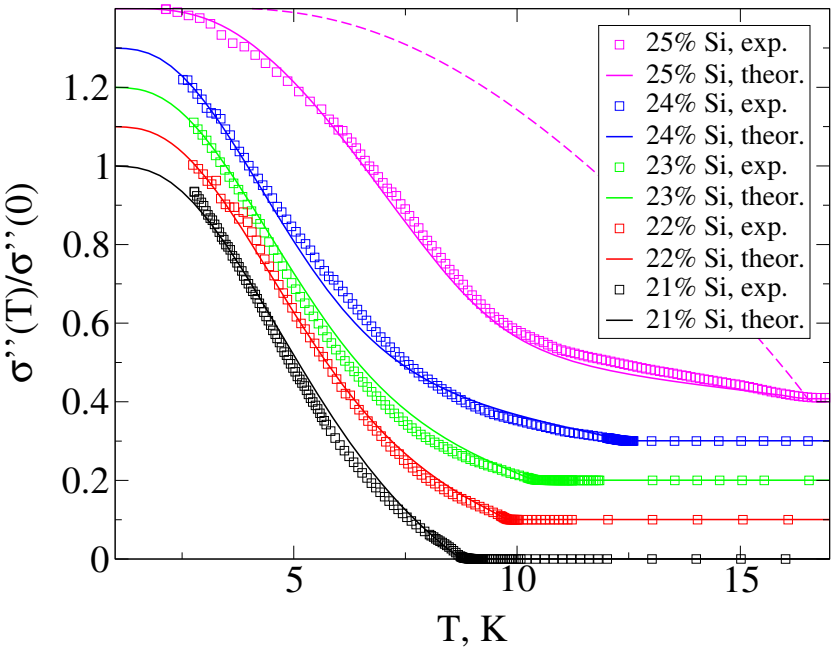

Fig. 6 The imaginary part of microwave conductivity in $V_{3+x}Si_{1-x}$ crystals in superconducting state. The *symbols* correspond to experimental data and the *solid lines* to calculations within the two-band model. For the sake of presentation clarity, each of the curves corresponding to 22% of Si and higher are shifted in the vertical direction by 0.1. *Dashed line* is calculation in the single-band BCS model

the stoichiometric one, reached their maximum values in the dirty limit. At the same time, the experimental data show approximately two times larger peak than theoretical calculation.

4 Conclusions

In conclusion, in this work, we have presented the results of the study of the temperature dependences of microwave conductivity in $V_{3+x}Si_{1-x}$ crystals with various Si content at frequency 9.4 GHz. The data exhibit peculiarities typical for multiband superconductors, namely nonlinear temperature dependence of resistivity above superconducting transition temperature T_c, suppression of T_c by nonmagnetic impurities, an upward curvature of $\sigma''(T)$ dependences near T_c, and a coherent peak of $\sigma'(T)$ at $T \sim T_c/2$. The data are interpreted within a two-band model in the weak-coupling regime. We have demonstrated that the behavior of T_c and the evolution of $\sigma(T)$ with Si-content variation are consistently described by the variation of the interband impurity scattering rate. The results strongly support the viewpoint that V_3Si belongs to the class of multiband superconductors.

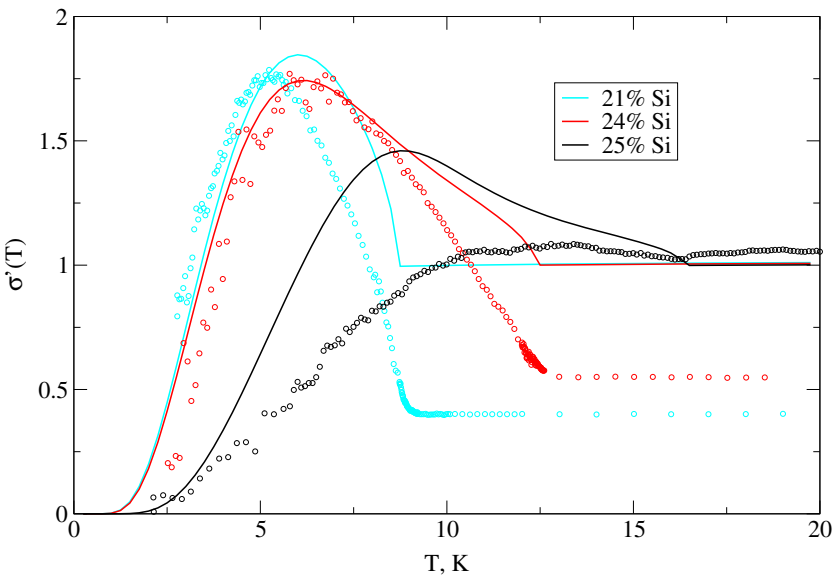

Fig. 7 The real part $\sigma'(T)/\sigma'(T_c)$) of microwave conductivity in superconducting state of $V_{3+x}Si_{1-x}$ crystals. The *solid lines* show the results of calculations within a two-band model of superconductivity. The *open circles* are the experimental data normalized in order to match the peak values of the calculated curves

Acknowledgments We would like to thank V.A. Marchenko for producing $V_{3+x}Si_{1-x}$ crystals. Helpful discussions with I.I. Mazin are gratefully acknowledged. This work was supported by mega-grant no.14Y26.31.0007 funded by Russian Ministry of Education and Science and in part by RFBR grant no.12-02-01009 and Dutch FOM.

References

1. Moskalenko, V.A.: Fiz. Met.Metalloved **8**(4), 503 (1959)
2. Moskalenko, V.A.: Phys. Met. Metallogr. **8**(4), 25 (1959)
3. Suhl, H., Matthias, B.T., Walker, L.R.: Phys. Rev. Lett **3**, 552 (1959)
4. Bardeen, J., Cooper, L.N., Schrieffer, J.R.: Phys. Rev **108**, 1175 (1957)
5. Shen, L.Y.L., Senozan, N.M., Phillips, N.E.: Phys. Rev. Lett. **14**, 1025 (1965)
6. Radebaugh, R., Keesom, P.H.: Phys. Rev. **149**, 209 (1966)
7. Hafstrom, J.W., MacVicar, M.L.A.: Phys. Rev. B **2**, 4511 (1970)
8. Binning, G., Baratoff, A., Hoenig, H.E., Bednorz, J.G.: Phys. Rev. Lett **45**, 1352 (1980)
9. Shulga, S.V., Drechsler, S.-L., Fuchs, G., Müller, K.-H., Krug, K.: Phys. Rev. Lett **80**, 1730 (1998)
10. Boaknin, E., Tanatar, M.A., Paglione, J., Hawthorn, D., Ronning, F., Hill, R.W., Sutherland, M., Taillefer, L., Sonier, J., Hayden, S.M., Brill, J.M.: Phys. Rev. Lett. **90**, 117003 (2003)
11. Wälte, A., Fuchs, G., Müller, K.-H., Handstein, A., Rosner, H.: Phys. Rev. B **70**, 174503 (2004)
12. Tanatar, M.A., Paglione, J., Nakatsuji, S., Hawthorn, D.G., Canfield, P.C., Fisk, Z.: Phys. Rev. Lett. **95**, 067002 (2005)
13. Bauer, E., Hilscher, G., Michor, H., Paul, Ch., Sigrist, M., Rogl, P.: Phys. Rev. Lett. **92**, 027003 (2004)
14. Guritanu, V., Goldacker, W., Bouquet, F., et al.: Phys. Rev. B **70**, 184526 (2004)
15. Hirschfeld, P.J., Korshunov, M.M., Mazin, I.I.: Rep. Prog. Phys. **74**, 124508 (2011)
16. Zehetmayer, M.: Supercond. Sci. Technol. **26**, 043001 (2013)
17. Nefyodov, Y.A., Shuvaev, A.M., Trunin, M.R.: Europhys. Lett. **72**, 638 (2005)
18. Kogan, V.G., Martin, C., Prozorov, R.: Phys. Rev. B **80**, 014507 (2009)
19. Perucchi, A., Nicoletti, D., Ortolani, M., et al.: Phys. Rev. B **81**, 092509 (2010)
20. Sonier, J.E., Callaghan, F.D., Miller, R.I., et al.: Phys. Rev. Lett. **93**, 017002 (2004)
21. Zehetmayer, M., Hecher, J.: Supercond. Sci. Technol. **27**, 044006 (2014)
22. Nam, S.B.: Phys. Rev **156**, 470 (1967)
23. Golubov, A.A., Mazin, I.I.: Phys. Rev. B **55**, 015146 (1997)
24. Golubov, A.A., Brinkman, A., Dolgov, O.V., et al.: Phys. Rev. B **66**, 054254 (2002)
25. Nicole, E.J., Carbotte, J.P.: Phys. Rev. B **71**, 054501 (2005)
26. Trunin, M.R.: J. Superconductivity **11**, 381 (1998)
27. Golubov, A.A., Dolgov, O.V., Boris, A.V., et al.: JETP Lett **94**, 333 (2011)